Quaternary Research 80 (2013) 33–46

Contents lists available at SciVerse ScienceDirect

Quaternary Research

journal homepage: www.elsevier.com/locate/yqres

Holocene reactivations of catastrophic complex flow-like landslides in the Flysch Carpathians (Czech Republic/Slovakia)

Tomáš Pánek [a,*], Veronika Smolková [a], Jan Hradecký [a], Ivo Baroň [b,1], Karel Šilhán [a]

[a] Department of Physical Geography and Geoecology, Faculty of Science, University of Ostrava, Chittussiho 10, 710 00 Ostrava, Czech Republic
[b] Czech Geological Survey, Brno branch, Leitnerova 22, 658 69 Brno, Czech Republic

ARTICLE INFO

Article history:
Received 4 October 2012
Available online 8 May 2013

Keywords:
Complex flow-like landslides
Landslide recurrence
Holocene
Flysch Carpathians

ABSTRACT

Complex flow-like landslides (CFLLs) are important geomorphic agents of Late Quaternary mountain evolution in the Flysch Belt of the Outer Western Carpathians. The CFLLs are characterised by the upper section of deep-seated, retrogressive landslide of structurally unfavourably oriented rocks and lower sections composed of earthflows originated due to liquefaction of material accumulated from the upper slopes. Radiocarbon dating of organic matter incorporated into landslide debris or related deposits suggests that most of the CFLLs collapsed repeatedly throughout the Holocene with typical recurrence intervals of approximately 1–2 ka. Catastrophic landslides that occurred during extreme hydrometeorological events in recent decades displayed evidence of Holocene activity. Most of the CFLLs dammed and steepened adjacent valleys. Our chronological dataset is biased by erosion of older landforms, but most of the dated reactivations correlate to regional increases in humidity identified by previous paleoenvironmetal studies.

Introduction

Recent field investigations in the Flysch Belt of the Outer Western Carpathians led to the discovery of several large rotational–translational slope failures that transformed into shallow earthflows at their frontal parts due to liquefaction of the substrate. These shallow landslides and earthflows are usually much faster and more destructive than their deep-seated precursors (Baroň et al., 2004, 2011; Klimeš et al., 2009). Here, we propose a new term for this type of slope failure — *complex flow-like landslides* (*CFLLs*). These failures are in accordance with complex landslides of Cruden and Varnes (1996), but by using this new term we put stress on the role of flow-type behaviour during landslide emplacement. The basal sliding zone of CFLLs crops out in the upper/middle parts of deformed slopes causing the slide material to liquefy and evolve into earthflows in their lower portion. In addition to representing hazard to local population and infrastructure (Evans et al., 2009), CFLLs are important Quaternary geomorphic agents responsible for the delivery of material into rivers, blocking valley floors in chronological orders of 10^3 to 10^4 yr and leaving conspicuous scars on mountain slopes (Korup et al., 2004, 2010; Baroň et al., 2011; Pánek et al., 2011a).

CFLLs extend over long distances and are characterised by high mobility and large volumes. Preserved deposits of ancient CFLLs in mountain terrains are useful for both determining landslide hazards and understanding Quaternary (especially Late Pleistocene–Holocene) geologic history. One aspect of landslide hazard assessment involves determining mass movement frequency on a given slope (Corominas and Moya, 2008). Despite recent progress in landslide hazard assessment based on historical records (Guzzetti et al., 2005) and improved dendrochronological techniques (Lopez Saez et al., 2012), these approaches only consider the latest episodes of slope evolution and may underestimate reactivation hazards of catastrophic landslides (Clague et al., 2003). Chronological investigation of landslides may thus provide information on past high-magnitude triggers, such as earthquakes or heavy rain falls. Although catastrophic landslides may not be strictly related to climatic factors (or widely, to any obvious triggering factor; e.g., Hancox et al., 2005), some chronological studies have revealed that landslides may be suitable paleoclimatological proxies (e.g., Soldati et al., 2004; Bookhagen et al., 2005; Dortch et al., 2009; Borgatti and Soldati, 2010).

In this study we focus on recent (i.e. defined here as originated since the beginning of 20th century) and Holocene CFLLs in the western Flysch Belt of the Outer Western Carpathians, especially in the eastern Czech Republic and western Slovakia. The causal factors of liquefaction on mountain slopes remain a subject for further research (Baroň et al., 2011). This paper focuses on dating large CFLLs in this area, evaluates their main geomorphic imprint and provides the first comprehensive data on their recurrence and Holocene history.

Regional settings

The western Flysch Belt of the Outer West Carpathians is located along the border of the Czech Republic and Slovakia (Fig. 1). These

* Corresponding author. Fax: +420 597 092 323.
E-mail address: tomas.panek@osu.cz (T. Pánek).
[1] Recent address: Geological Survey of Austria, Neulinggasse 38, 1030 Vienna, Austria.

0033-5894/$ – see front matter © 2013 University of Washington. Published by Elsevier Inc. All rights reserved.
http://dx.doi.org/10.1016/j.yqres.2013.03.009

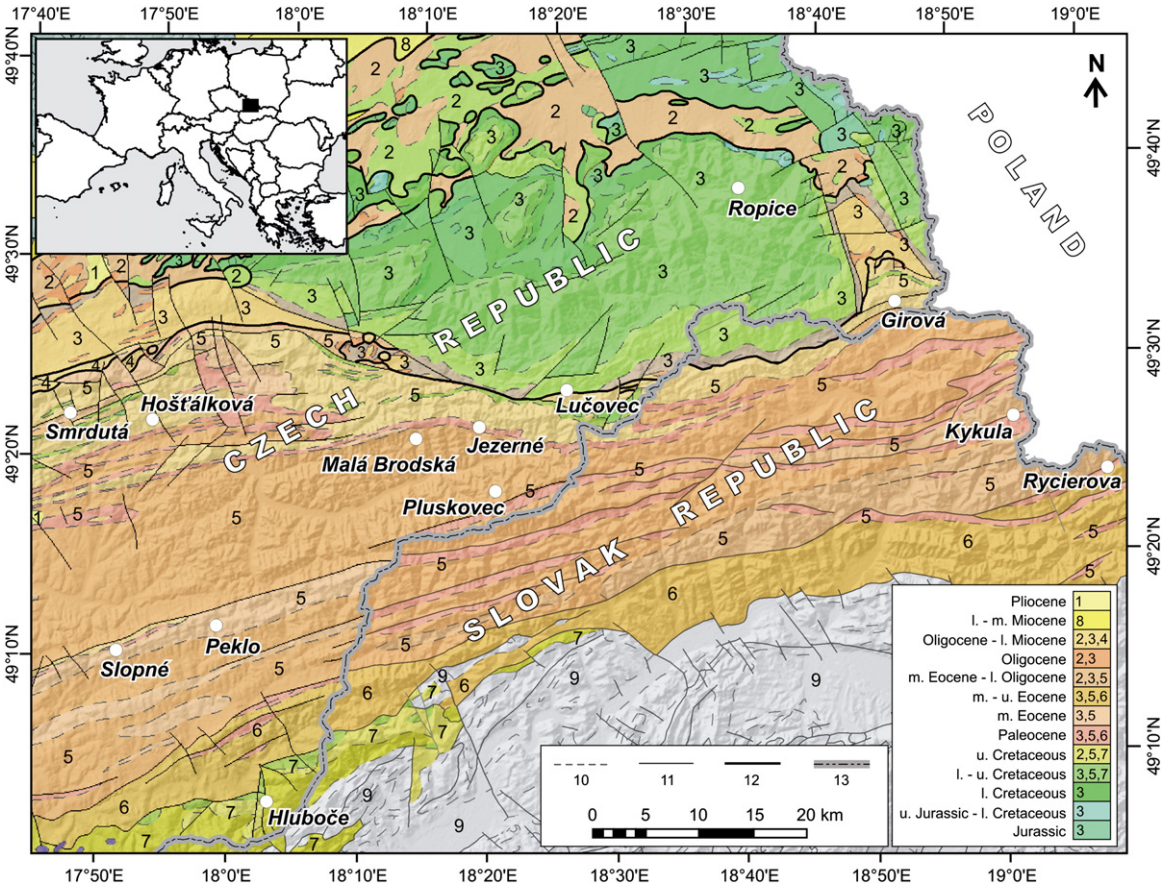

Figure 1. Geology of the study area with locations of the studied CFLLs (white dots): (1) postorogenic sediments (Pliocene); (2) flysch formations of the Subsilesian Unit (Outer Group of Nappes, upper Cretaceous–lower Miocene); (3) flysch formations of the Silesian Unit (Outer Group of Nappes, upper Jurassic–lower Miocene); (4) flysch formations of the Fore-Magura Unit (Outer Group of Nappes, upper Cretaceous–lower Miocene); (5) flysch formations of the Raca Unit (Magura Group of Nappes, lower Cretaceous–lower Oligocene); (6) flysch formations of the Bystrica Unit (Magura Group of Nappes, Paleogene–Eocene); (7) flysch formations of the Bile Karpaty Unit (Magura Group of Nappes, upper Cretaceous–Paleogene, with middle Miocene volcanism); (8) sediments of the Carpathian Neogene foredeep (lower to middle Miocene); (9) Pieniny Klippen Belt and Inner Western Carpathians; (10) lithological boundaries; (11) faults; (12) main thrust faults; and (13) state boundaries.
Source: Biely (1996), Cháb et al. (2007); elevation data: SRTM3 v.2.

mountains have a fold-and-thrust structure consisting mostly of Cretaceous and Paleogene shales, claystones and sandstones, which were thrusted during the Paleogene and Neogene over the Northern European platform and part of its foredeep (Picha et al., 2006). The region is divided into two major nappe groups (Fig. 1). Most of the territory in the south and east is composed of Magura Nappe, which is an intensively folded structure characterised by alternating WSW–ESE striking flysch beds. The northeast area (i.e., Moravskoslezské Beskydy Mts.) is characterised by the less folded, nearly monoclinal structure of the Silesian Nappe, generally dipping towards the S and SE. Flysch bedrock is very anisotropic due to the lithological contrast of competent sandstones and conglomerates versus incompetent shales and claystones and dense jointing. Faults striking in E–W to NE–SW directions represent mainly regional thrusts; transverse discontinuities with directions NW–SE to NNE–SSW are usually related to strike-slip and normal faults. The maximum elevation of the study area is 1323 m asl, with the local relief up to 750 m km^{-1}. The current seismicity of the area is relatively low (Lenhardt et al., 2007). Apatite fission track and (U–Th)/He thermochronology indicate that recent gross landforms of the Flysch Carpathians are not older than ~9 Ma (Danišík et al., 2008; Zattin et al., 2011). Recent annual precipitation totals vary between 900 and 1500 mm, with higher amounts at higher altitudes in the NE part of the region.

Anisotropic flysch is prone to deep-seated mass movements, especially due to elevated pore-water pressures during extreme hydrometeorological events, such as heavy rain falls and rapid snowmelt (Krejčí et al., 2002; Baroň et al., 2005; Margielewski, 2006a). To this date, >5800 landslides have been inventoried within the Czech part of the Flysch Belt of the Outer West Carpathians (Baroň et al., 2004), and approximately 4600 landslides have been inventoried in the West Slovakian part (Šimeková and Martinčeková, 2006). The study area was not glaciated during the Pleistocene, hence the landslides, as well as rivers, can be considered to be the most important Quaternary geomorphic agents influencing landscape denudation, namely via the lowering and disruption of mountain ridges (Pánek et al., 2011b) or erosion and accumulation processes within valley slopes and floors (Baroň et al., 2010; Pánek et al., 2010). Landslide-related peat bogs are often the only suitable sources of late Quaternary paleoenvironmental records in the region (Margielewski, 2006a; Margielewski et al., 2010).

Methods

This study presents new data and reviews previously published information (Baroň, 2007; Klimeš et al., 2009; Pánek et al., 2009a,b, 2010; Baroň et al., 2011; Pánek et al., 2011a, 2013) on the age and recurrence of thirteen large Holocene and recent CFLLs in the western Flysch Belt of the Outer Western Carpathians (Fig. 1; Table 1). Geomorphic analyses involved mapping landslide deposits in the field and on aerial photographs at a scale of 1:5000. The volume of individual landslides was estimated using empirical volume-area scaling relationships (Guzzetti et al., 2009), which are commonly used for

https://doi.org/10.1016/j.yqres.2013.03.009 Published online by Cambridge University Press

Table 1
Morphometric and other relevant characteristics of the studied landslides. Individual CFLLs are ordered according to the age of oldest activation.

Landslide name	Location	Area[a] (km^2)	Volume[a] ($\times 10^6$ m^3)	Length[a] (L, m)	Width[a] (W, m)	Height[a] (H, m)	H/L	Age/recurrence	Comment	Reference
Kykula	49.440°N 18.961°E	1.50	12.0	2950	780	420	0.14	Several (at least two) activations between ca 11.5–9.4 cal ka BP.	Translational landslide/earthflow predisposed by bedding planes and thrust faults. Retrogressive behaviour.	Pánek et al. (2010)
Peklo	49.205°N 18.968°E	0.16	2.2	970	210	195	0.20	Four activations dated to ca 7.2, 6.4, 4.5 and 0.6 cal ka BP.	Rotational–translational landslide/earthflow, partly predisposed by fault/joint planes.	This study
Girová	49.528°N 18.792°E	0.51 *0.20*	8.8 *2.5*	1530 *1150*	650 *300*	275 *170*	0.18 *0.15*	Catastrophic landslide evolved during 19–22 May 2010. Three instabilities dated to ca 7.5, 1.5, and 0.6 cal ka BP preceded recent event.	Translational landslide/earthflow, wedge-like headscarp predisposed by the intersection of steep deep-weathered fault zones. Retrogressive behaviour.	Pánek et al. (2011a)
Smrdutá	49.373°N 17.753°E	0.06	0.7	670	115	225	0.33	Three activations dated to ca 4.6, 2.0, and 0.3 cal ka BP.	Rockslide with some boulders 15 m across, several generations of headscarps predisposed by joints and bedding planes.	Pánek et al. (2013)
Slopné	49.176°N 17.834°E	0.05	0.5	470	130	95	0.20	Landslide dated to ca 1.6 cal ka BP, minor recent instabilities within the landslide body.	Rotational–translational landslide/earthflow, wedge-like headscarp predisposed by the intersection of steep bedding planes and joints.	This study
Lučovec	49.425°N 18.387°E	0.13	1.7	600	250	125	0.21	Two successive landslides evolved during a short time interval between ca 1.3–1.7 cal ka BP. Possible younger retrogressive shift of headscarp ca 0.7 cal ka BP.	Rotational–translational landslide/earthflow partly predisposed by fault. Retrogressive behaviour.	This study and Pánek et al. (2009a)
Hošťálková	49.370°N 17.856°E	0.22	3.3	750	300	130	0.17	Catastrophic landslide evolved during 12–13 January 1919. At least one landslide dated to ca 1.4 cal ka BP preceded recent event.	Rotational landslide/earthflow predisposed by 250–300 m wide, deeply weathered fault zone.	This study
Ropice	49.603°N 18.583°E	0.38	0.8	1020	150	250	0.25	Rockslide dated to ca 1.3 cal ka BP, possible reactivation ca 0.4 cal ka BP.	Rockslide with some boulders 10 m across predisposed by fault plane parallel with the slope surface. Nested within large deep-seated slope failure with signs of sackung.	Pánek et al. (2009b)
Hluboče	49.064°N 18.052°E	*0.06*	*0.1*	*770*	*110*	*186*	*0.24*	Catastrophic landslide originated during 3–4 April 2006. At least one landslide dated to ca 1.3 cal ka BP preceded the recent event.	Rotational–translational landslide/earthflow, nested within a deeply weathered fault zone.	Klimeš et al. (2009)
Malá Brodská	49.376°N 18.202°E	*0.03*	*0.3*	*685*	*90*	*175*	*0.26*	Catastrophic landslide originated on 7th July 1997. At least one landslide dated to ca 1.1 cal ka BP preceded the recent event.	Wedge-like landslide/earthflow strongly predisposed by the intersection of bedding planes and fault. Nested within a larger deep-seated slope failure.	This study
Jezerné	49.390°N 18.272°E	0.06	0.6	690	100	185	0.27	Rockslide dated to ca 0.8 cal ka BP, possibility of earlier long-runout landslides.	Partly predisposed by steep bedding planes forming conditions for wedge-like failure. Situated within a large deep-seated slope failure.	This study
Rycierova	49.406°N 19.094°E	0.30	4.6	1600	280	380	0.24	Rockslide dated to ca 1.0 cal ka BP, possibility of earlier long-runout landslides.	Wedge-like rockslide predisposed by the intersection of two joint sets and bedding planes. Some boulders are more than 10 m across. Situated within a large deep-seated slope failure with signs of sackung.	This study
Pluskovec	49.337°N 18.305°E	0.11	1.4	745	260	170	0.23	Last landslide dated to ca 0.9 cal ka BP. Possibility of older instabilities.	Wedge-like rotational–translational landslide predisposed by the intersection of steep bedding planes and joints.	This study

[a] Landslide dimensions are calculated as cummulative, involving all reactivations. Italics denote dimensions of known recent catastrophic landslide events.

landslides with areas ranging from 6×10^3 to 6×10^7 m^2. Most of the CFLLs are composite landforms resulting from long-term, repeated activity, so precise volumetric determination of individual landslide generations is difficult. We therefore present total cumulative landslide volumes. Volumes of individual landslide generations were stated only for some recent catastrophic events and morphologically well-defined older generations (Table 1).

Structural conditions in the vicinity of the landslides (especially in headscarp areas) were evaluated by measurements of main discontinuity sets, and their interactions with slope geometry and possible

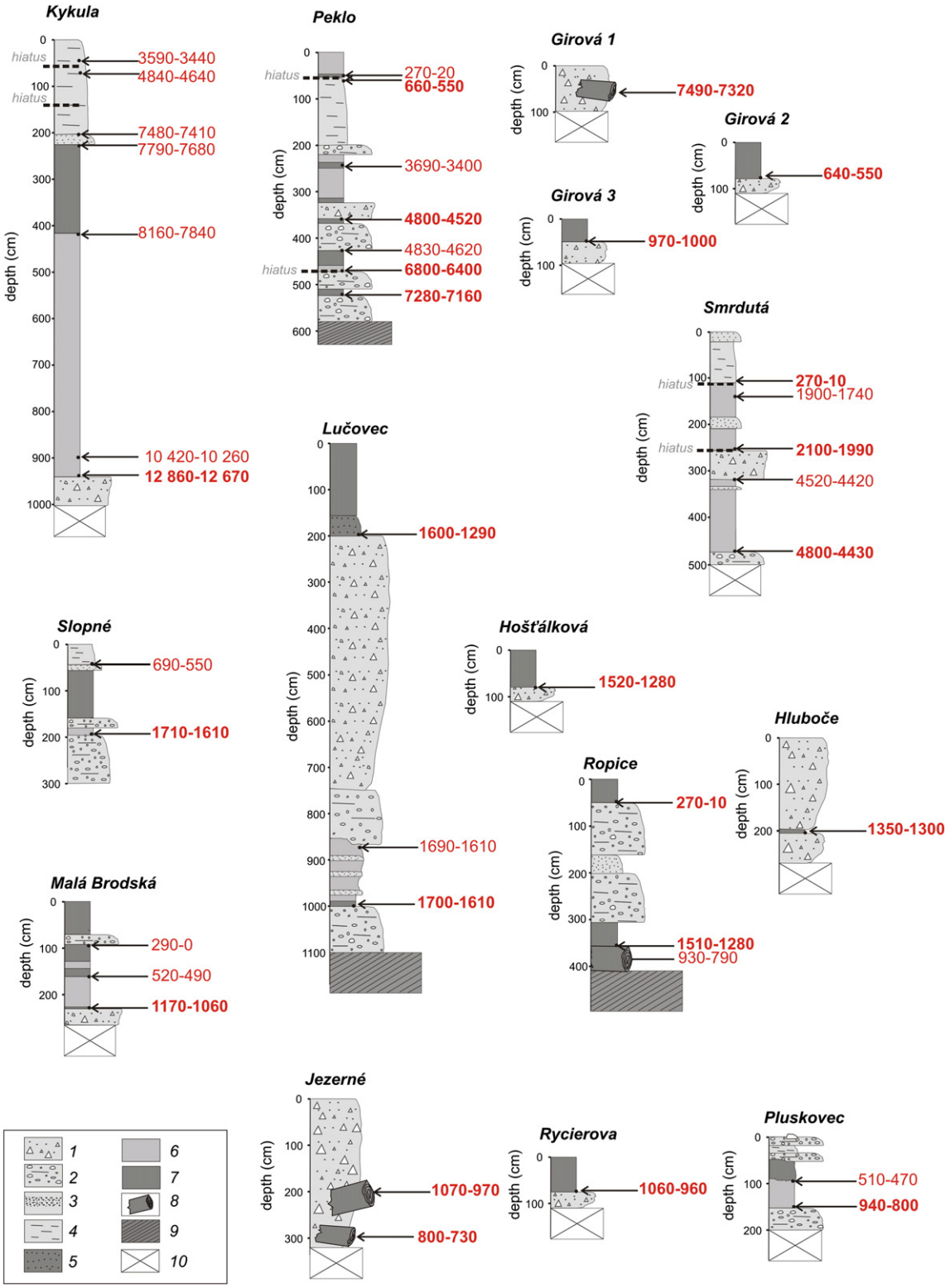

Figure 2. Lithostratigraphic sections used to determine ages and recurrences of individual landslides. Ages approximating the time of landslide origin/reactivations are bolded. Radiocarbon ages (1σ range; see Table 2) are expressed in cal yr BP. (1) landslide diamict; (2) alluvial gravels; (3) alluvial sands; (4) alluvial loams (sandy silts, clays); (5) organic silts and clays (gyttja) contaminated by gravels and sands; (6) lacustrine silts and clays; (7) organic silts and clays (gyttja); (8) buried tree trunks; (9) flysch bedrock; (10) unavailable sections.

https://doi.org/10.1016/j.yqres.2013.03.009 Published online by Cambridge University Press

Table 2
Radiocarbon data for the studied landslide events and related sedimentary bodies.

Landslide/depth (cm)	Laboratory number	Dated material	^{14}C Age (^{14}C yr BP)	1σ range cal yr BP[a]	Context of dating	Reference
Kykula						
940	GdA-1179[b]	Organic mud	10,900 ± 60	**12,860–12,670**	Base of dammed lake/origin of landslide	Pánek et al. (2010)
895	GdA-1180[b]	Wood	9205 ± 45	10,420–10,260	Landslide-dammed lake deposits (>3 m deep lake)	Pánek et al. (2010)
415	Gd-19 124[c]	Wood	7140 ± 110	8160–7840	Start of peaty gyttja sedimentation (shallow lake)	Pánek et al. (2010)
225	GdA-1183[b]	Organic mud	6900 ± 40	7790–7680	Termination of deposition within landslide-dammed lake/swamp	Pánek et al. (2010)
180	GdA-1184[b]	Wood	6520 ± 40	7480–7410	Sandy inclusion (alluvial sedimentation)	Pánek et al. (2010)
75	GdA-1350[b]	Organic mud	4185 ± 35	4840–4640	Base of overbank deposits (alluvial sedimentation)	Pánek et al. (2010)
45	Gd-20 000[c]	Wood	3290 ± 60	3590–3440	Overbank deposits (alluvial sedimentation)	Pánek et al. (2010)
220	GdA-1351[b]	Detritus	8360 ± 50	**9470–9300**	Base of peat bog overlying near-scarp depression in the upper part of landslide/approximate age of landslide reactivation	Pánek et al. (2010)
Girová						
50–100	Beta-288258[c]	Wood/trunk	6510 ± 60	**7490–7320**	Trunk buried within landslide deposits/origin of long-runout landslide (landslide activity preceding catastrophic landslide from May 2010)	Pánek et al. (2011a)
0	Ki-16615[c]	Wood	5910 ± 120	6900–6560	Trunk buried within landslide deposits exposed by a recent phase from May 2010	Baroň et al. (2011)
70	GdA-1978[b]	Needles	1640 ± 20	**1560–1520**	Basal part of peat bog overlying landslide/probable minor activation of the upper part of the landslide area (landslide activity preceding the catastrophic landslide of May 2010)	Pánek et al. (2011a)
56	GdA-1979[b]	Needles	590 ± 20	**640–550**	Basal part of peat bog overlying landslide/probable minor activation of the upper part of landslide area (landslide activity preceding the catastrophic landslide of May 2010)	Pánek et al. (2011a)
Peklo						
526	GdA-1356[b]	Detritus	6310 ± 50	**7280–7160**	Base of shallow landslide-dammed lake/origin of landslide	This study
464	Gd-30 205[c]	Leaves	5800 ± 170	**6800–6400**	Base of shallow landslide-dammed lake/reactivation of landslide	This study
426	GdA-1357[b]	Detritus	4160 ± 40	4830–4620	Termination of shallow landslide-dammed lake sedimentation	This study
360	GdA-1359[b]	Organic mud	4090 ± 40	**4800–4520**	Thin layer of dammed deposits/reactivation of landslide	This study
270	Gd-19 232[c]	Detritus	3310 ± 110	3690–3400	Deposits of shallow landslide-dammed lake	This study
70	GdA-1360[b]	Detritus	620 ± 30	**660–550**	Base of shallow landslide-dammed lake/reactivation of landslide	This study
40	Gd-19 254[c]	Plant detritus	75 ± 90	270–20	Deposits of shallow landslide-dammed lake/swamp	This study
Smrdutá						
473	GdS-1094[c]	Wood	4065 ± 80	**4800–4430**	Base of shallow landslide-dammed lake/origin of landslide	Pánek et al. (2013)
385	GdA-1996[b]	Leaf	3990 ± 30	4520–4420	Erosional top of shallow landslide-dammed lake deposits	Pánek et al. (2013)
257	GdA-1997[b]	Piece of plant	2075 ± 20	**2100–1990**	Base of shallow landslide-dammed lake/reactivation of landslide	Pánek et al. (2013)
143	UGAMS[b] 8590	*Coleoptera* fragment	1900 ± 40	1900–1740	Erosional top of shallow landslide-dammed lake deposits	Pánek et al. (2013)
101	GdA-2000[b]	Piece of cone	130 ± 30	**270–10**	Base of alluvial overbank sedimentation/possibly impounded by landslide reactivation	Pánek et al. (2013)
Slopné						
196	GdA-1362[b]	Plant detritus	1745 ± 30	**1710–1610**	Base of shallow landslide-dammed lake/origin of landslide	This study
48	Gd-19 218[c]	Plant detritus	670 ± 90	690–550	Base of alluvial overbank sedimentation	This study
Lučovec						
1000	UGAMS[b] 9630	Needles	1740 ± 25	**1700–1610**	Base of shallow landslide-dammed lake/first generation of landslide	This study
860	UGAMS[b] 9631	Needles	1700 ± 25	1690–1550	Erosional top of shallow landslide-dammed lake deposits	This study
200	Ki-13 709[c]	Plant detritus	1540 ± 150	**1600–1290**	Basal part of peat bog overlying landslide toe/second generation of landslide	Pánek et al. (2009a)
200	Ki-13 700[c]	Plant detritus	820 ± 140	**910–660**	Basal part of peat bog overlying near-scarp depression of landslide/retrogressive reactivation of the upper part of the landslide	Pánek et al. (2009a)
Hošťálková						
80	IGSB-1066[c]	Wood	1460 ± 100	**1520–1280**	Basal part of peat bog overlying near-scarp depression of the landslide (landslide activity preceding the catastrophic landslide of January 1919)	Baroň (2007)
Ropice						
400	Ki-13 717[c]	Wood/trunk	950 ± 60	930–790	Possibly younger fallen tree trunk which penetrated to the older lacustrine/palustrine deposits	Pánek et al. (2009b)

(continued on next page)

https://doi.org/10.1016/j.yqres.2013.03.009 Published online by Cambridge University Press

Table 2 (*continued*)

Landslide/depth (cm)	Laboratory number	Dated material	^{14}C Age (^{14}C yr BP)	1σ range cal yr BP[a]	Context of dating	Reference
Ropice						
355	Ki-13 714[c]	Peat	1450 ± 100	**1510–1280**	Base of shallow landslide-dammed lake/first generation of rockslide	Pánek et al. (2009b)
170	Ki-12 658[c]	Plant detritus	310 ± 60	**460–300**	Base of second generation of backwater dammed deposits/second generation of rockslide	Pánek et al. (2009b)
50	Ki-13 711[c]	Peat	130 ± 50	270–10	Base of peat bog which terminates deposition within landslide-dammed impoundment	Pánek et al. (2009b)
Hluboče						
200	GdA-1348[b]	Charcoal	1435 ± 30	**1350–1300**	Soil buried by landslide toe (landslide activity preceding the catastrophic landslide of April 2006)	Klimeš et al. (2009)
Malá Brodská						
224	UGAMS[b] 9244	Needles	1180 ± 25	**1170–1060**	Base of shallow landslide-dammed lake (landslide preceding the catastrophic failure of July 1997)	This study
160	UGAMS[b] 9247	*Coleoptera* fragment	440 ± 25	520–490	Deposits of shallow landslide-dammed lake	This study
88	UGAMS[b] 9246	Needles	160 ± 25	290–0	Deposits of shallow landslide-dammed lake	This study
Jezerné						
~300	Ki-14 046[c]	Outer tree-ring of trunk	860 ± 30	**800–730**	Trunk within rockslide deposits	This study
~200	Ki-14 047[c]	Outer tree-ring of trunk	1120 ± 40	**1070–970**	Trunk within rockslide deposits (likely redeposited from older accumulation)	This study
Rycierova						
75	UGAMS[b] 9254	Needles	1100 ± 20	**1060–960**	Base of the peat bog overlying landslide toe	This study
Pluskovec						
155	UGAMS[b] 9243	Needles	980 ± 25	**940–800**	Base of shallow landslide-dammed lake	This study
90	UGAMS[b] 9242	Wood	410 ± 25	510–470	Erosional top of shallow landslide-dammed lake deposits	This study

[a] Ages representing origin/reactivation of landslides are shown in bold.
[b] Accelerator mass spectrometry method.
[c] Liquid scintillation counting method.

kinematics of landslide movements (Brideau et al., 2009) were analysed. The imprint of individual landslides on the topography of adjacent valley floors was evaluated by calculating the steepness index of individual rivers (k_s; for calculation see Flint, 1974; Whipple, 2004; Korup, 2006) using a fixed concavity index ($\theta = 0.3$) and 5-m DEM. Application of k_s enables assessment of the long-term influence of slope failures on the local gradient of valley floors (e.g., Korup, 2006).

The age of landslides was investigated by radiocarbon dating of organic material obtained directly from the landslide debris or, more frequently, from related lacustrine or fluvio-lacustrine sediments (i.e., deposits of dammed lakes or peat bogs on the surface of landslides) (Lang et al., 1999; Bertolini et al., 2004; Soldati et al., 2004). In our study, representative samples for ages of individual landslides or their reactivations were those embedded within landslide debris or situated at the bottom of lacustrine or peat bog deposits (Fig. 2). Deposits in dammed paleolakes and landslide peat bogs were analysed from natural outcrops or extracted using a percussion Eijkelkamp sampler with a synthetic foil liner (63 mm diameter) and Russian peat sampler (60 mm diameter). Uncertainties in our dating technique may have led to both over- and under-estimation of the timing of landslides. For example, the age of organic material incorporated within landslide debris may be older than a particular landslide due to multiple resedimentation and/or reactivation. In contrast, the ages of sediment trapped within dammed lakes and landslide peat bogs are younger than a particular slope failure. Despite these uncertainties, we suppose that our dating strategy is suitable and as it has been demonstrated by numerous recent studies (e.g., Bookhagen et al., 2005; Margielewski, 2006a; Prager et al., 2009; Margielewski et al., 2010), especially basal ages of dammed lacustrine sequences well reflect the ages of particular landslides.

Together, 25 radiocarbon dates (mainly AMS) define the origin or reactivation of individual landslides, and numerous other ages are presented to define other important processes connected to the evolution of landslides (e.g., duration of landslide dams, etc.). Radiocarbon dating was carried out at the Gliwice Radiocarbon Laboratory of the Institute of Physics, Silesian University of Technology (Poland; samples marked as GdA/Gd, Table 2), University of Georgia, Centre for Applied Isotope Studies (USA; samples marked as UGAMS, Table 2), Kyiv Radiocarbon Laboratory (Ukraine; samples marked as Ki, Table 2) and Minsk University (Belarus; one sample marked as IGSB in Table 2). Raw ^{14}C dates were converted into calendar ages using the IntCal 09 calibration curve (Reimer et al., 2009) in OxCal v 4.1.7 software (Bronk Ramsey, 2009; Table 2). In the text, we express calibrated ages in their one-sigma ranges. For comparison with other regional paleoenvironmental proxies, dated CFLLs were plotted against reconstructed probability density curves from earlier ^{14}C dated landslides from both Czech and Polish parts of the Flysch Western Carpathians (Alexandrowicz and Alexandrowicz, 1999; Margielewski, 2006a; Baroň, 2007; Margielewski et al., 2010, 2011) and paleoflood events for the nearby Polish territory (Starkel et al., 2006) as well as other Central European paleoclimate proxies (Niggemann et al., 2003; Magny, 2004; Starkel et al., 2006).

Results

General features and overview of studied CFLLs

CFLLs in the study area comprise a diverse spectrum of slope failures extending over relatively long distances (470–2950 m) and are characteristic of high mobility (10^{-1}–10^{2} m/day as stated for recent events), high volumes (0.1–12 × 10^{6} m^3) and significant liquefaction

https://doi.org/10.1016/j.yqres.2013.03.009 Published online by Cambridge University Press

of the displaced material in their middle to lower portions. The main characteristics of studied landslides are presented in Table 1.

The largest group of CFLLs includes older (Kykula, Peklo, Slopné, Lučovec, Pluskovec), and recent catastrophic failures (Girová, Hošťálková, Hluboče, Malá Brodská) which originated mainly within rock massifs containing a significant fraction of weak claystone/mudstone-dominated flysch. Failures in this group are rotational–translational or purely translational landslides combined with distal earthflows (Table 1; Figs. 3 and 4). Distinct long-runout toes contrast with upper slope portions formed by short-displacement, deep-seated gravitational slope failures (Figs. 3 and

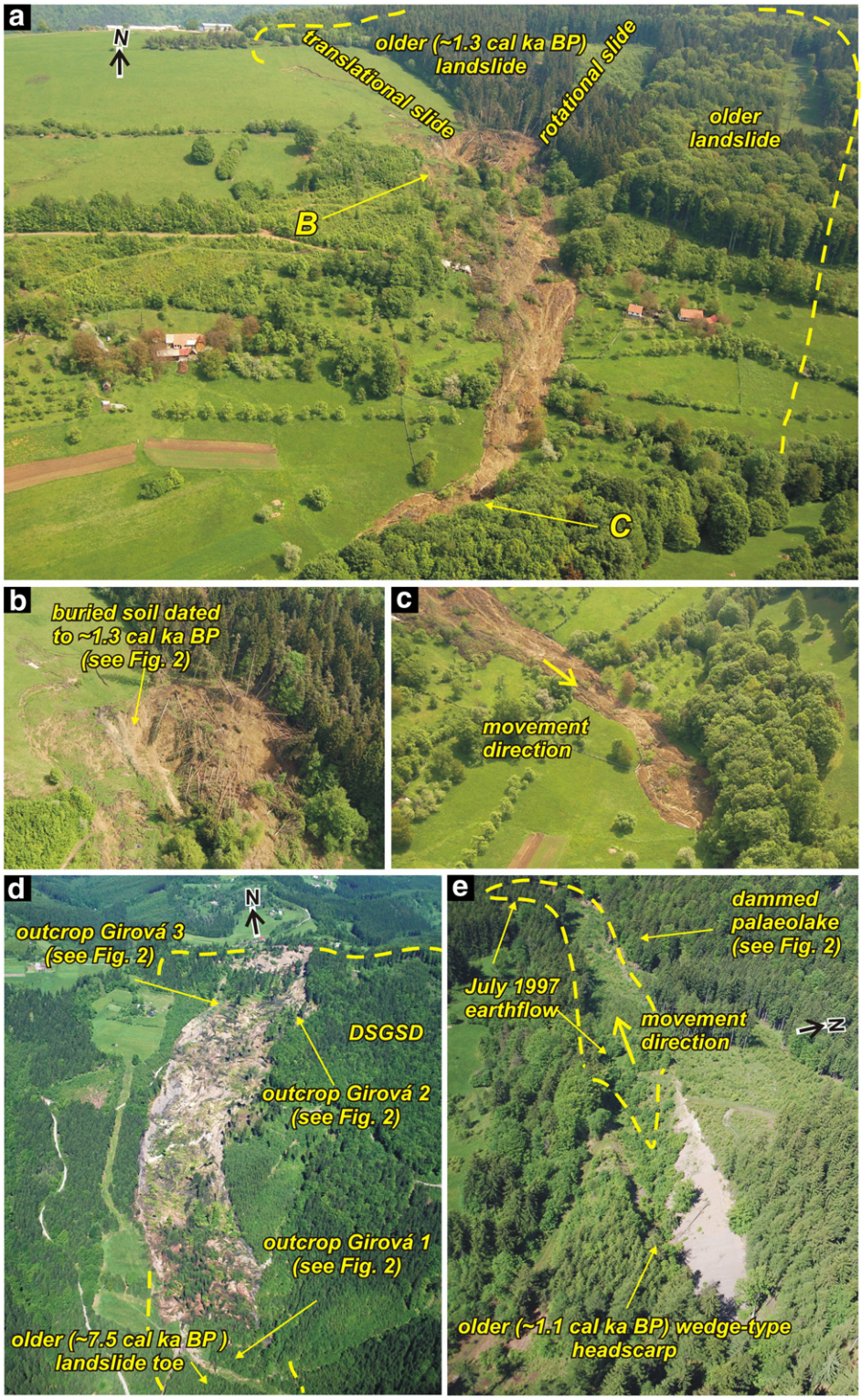

Figure 3. Features of selected, recent CFLLs demonstrated by oblique airborne photos. a. The Hluboče CFLL in March 2006 near Brumov Bylnice after heavy rainfall and sudden snow-thaw; a translational landslide and mainly rotational and deep-seated in a much larger and older DSGSD, transformed into an earthflow, which destroyed five houses. b. Detail of the transformation zone into the earthflow. c. The accumulation of the same earthflow. d. The Girová CFLL activated after intense rainfalls in May 2010 within a DSGSD. e. The Malá Brodská landslide represents a reactivated wedge failure, which transformed into an earthflow after heavy rainfalls in July 1997. The photos document significant liquefaction on the slopes related to the activity of upper, deep-seated landslides (all photos by I. Baroň).

https://doi.org/10.1016/j.yqres.2013.03.009 Published online by Cambridge University Press

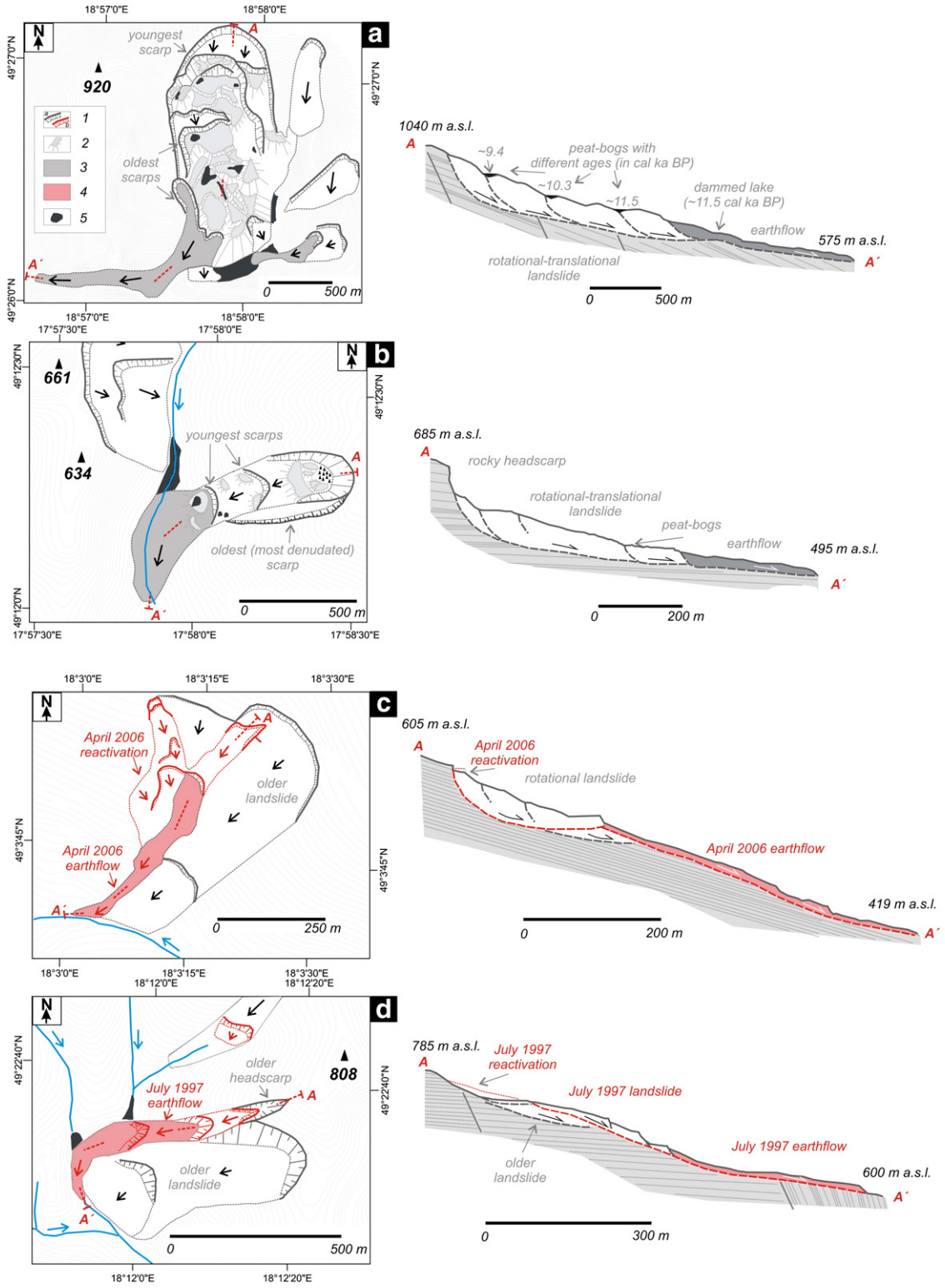

Figure 4. Cross-sections of typical CFLLs demonstrating the relationship between upper, deep-seated deformations and distal liquefied portions. a. Kykula landslide. b. Peklo landslide. c. Hluboče landslide, d. Malá Brodská landslide (1) scarps (a — old, b — recent); (2) landslide blocks; (3) liquefied old earthflow accumulations; (4) liquefied recent earthflow accumulations; (4) peat bogs and impounded sections of floodplains.

4). Some of these lobes are associated with movements of wedge-type blocks of relatively simple geometry (Slopné, Pluskovec, Girová, Malá Brodská), and the rest of the failures originated at the foot of a complex system of numerous rotated and/or translated deep-seated blocks (Peklo, Lučovec, Girová, Hošťálková, Hluboče) (Figs. 3 and 4). Examples of recent catastrophic failures include the January 1919 Hošťálková landslide, July 1997 Malá Brodská landslide, April 2006 Hluboče landslide and the May 2010 Girová landslide; these are examples of CFLLs in older landslide terrains with recurrent behaviour.

Another group of CFLLs (Smrdutá, Ropice, Rycierova, and Jezerné) is characterised by rockslides affecting predominantly competent sandstone beds. These failures have distal, up to 1 km long tongues bearing pronounced stony accumulations, with sandstone blocks sometimes exceeding 10 m in the a-axis (Fig. 5). High mobility and

https://doi.org/10.1016/j.yqres.2013.03.009 Published online by Cambridge University Press

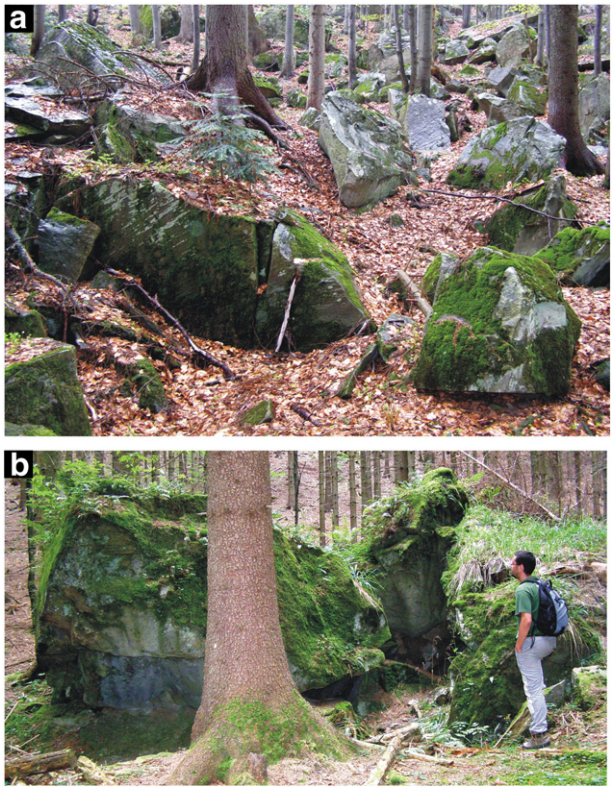

Figure 5. Stony accumulations with sandstone blocks exceeding 10 m are characteristic features for some distal liquefied parts of rockslides. a. Rycierova rockslide. b. Jezerné rockslide.

relatively long runout of the CFLL lobes were also likely facilitated by the liquefaction of slope substratum in the outcrop zone of basal shear surfaces in the middle parts of slopes. This process is exemplified by the Rycierova landslide, which is the largest slope failure in this category (Table 1, Fig. 5).

Geological predispositions of CFLLs

Most of the CFLLs are spatially related to deep-seated gravitational slope deformations (DSGSDs) situated along tectonic discontinuities and tectonically weakened zones within flysch rock masses (Figs. 3 and 4).

Structurally predisposed slope deformations involve wedge-type failures originating at the intersection of two or more discontinuity sets, such as two conjugate fault planes (e.g., Girová landslide), fault (joint) × bedding plane (e.g., Malá Brodská landslide) and two joint systems (e.g., Rycierova landslide) (Fig. 6). These landslides have triangle-shaped depletion zones in planform view, and most of their courses are strongly aligned along major structural discontinuities. Tectonic zones of reduced strength enable periodic reactivations of slope failures accompanied by headscarp retrogressions (Fig. 6).

Some of the recent catastrophic landslides (January 1919 Hošťálková and April 2006 Hluboče landslides) together with ancient Lučovec recurrent failure are predisposed by strongly fractured tectonic shear zones, reaching a width up to several hundreds of metres (Table 1; Fig. 6). These continuous major deformed zones often transverse opposing mountain ridges. They nest numerous slope deformations successively arranged across drainage divides. Landslides predisposed by such weakened zones usually lack structurally predisposed slip surfaces. Instead, they have rotational shear surfaces, which are typical of isotropic materials with significantly reduced shear strength (Margielewski, 2006b).

Apart from failures aligned with the strike of bedrock discontinuities, we can also distinguish landslides that originated perpendicularly to the strike of major discontinuities. This is the case of the Kykula, Ropice or Smrdutá failures, perpendicularly evacuating tectonically jointed and/or faulted sandstone-dominated bedrock (Table 1; Fig. 6).

Age and recurrence of CFLLs

The morphology of CFLLs clearly shows the recurrent nature of failures given by numerous generations of scarps and distal lobes (Fig. 4). The ages of CFLLs from our dataset span the entire Holocene period, with a strong bias towards the youngest, Subatlantic chronozone (Table 2; Fig. 2). The oldest landslide (Kykula) originated in the Younger Dryas/Holocene transition (11.5–9.4 cal ka BP), and the youngest reactivation (excluding modern catastrophic failures) was identified within the Little Ice Age period (Smrdutá landslide, ca. 0.3 cal ka BP). One of the largest CFLLs (Girová landslide) originated during the May 2010 extreme rainfall event. Most of the dated landslides (75%) originated during the last 2000 years, with a pronounced cluster between ca. 1.7 and 1 cal ka BP (34% of all dated activations). Some individual events were dated to the Atlantic chronozone (7.4–6.6 cal ka BP; Girová and Peklo landslides) and the beginning of the Subboreal chronozone (ca. 4.6 cal ka BP; Smrdutá and Peklo landslides).

One of the most important findings of this study is that most CFLLs are recurrent phenomena. For instance, the Peklo landslide contains four scarps characterised by different degrees of denudation, suggesting multistage evolution (Fig. 4). This is supported by four generations of fluvio-lacustrine sediments in adjacent dammed paleolake dated to 7.2, 6.4, 4.5 and 0.6 cal ka BP (Table 1, Fig. 4). Generally, we can identify two chronological types of recurrences — successive major activations separated by short chronological intervals (up to several centuries; e.g., Kykula or Lučovec), and repeated major movements after relatively long periods spanning more than one millennium (e.g., Malá Brodská landslide). Some failures from the latter group were reactivated several times throughout the Holocene (e.g., Peklo and Girová landslides).

The ^{14}C geochronology data are not fully sufficient for determining recurrence intervals of all slope failures (we were not able to detect some activations by dating), so we can only estimate maximum recurrence intervals for major reactivations for eight well-dated CFLLs (Table 3). The average recurrence interval for these landslides was 1.45 ± 0.7 ka (ranges from 0.3 to 2.5 ka for the Jezerné and Girová landslides, respectively) (Table 3). However, average recurrence intervals can be misleading, especially for landslides with highly asymmetrical temporal distributions. For instance, the Girová landslide reveals a pronounced cluster of events from ca. 1.5 cal ka BP to modern times (three events, including the May 2010 catastrophic failure), which followed ca. 5.9 ka of a relative slope stability (Pánek et al., 2011a).

Imprint of CFLLs on valley floors

The liquefied and relatively long-runout slope failures reached valley floors and affected the geomorphic regime of mountain rivers. Except for two cases, all landslides in our dataset blocked valley floors and influenced steepness parameters of river profiles (Fig. 7). Sedimentological and pollen indices show that the longevity of landslide-dammed lakes before breaching of dams spanned a variety of times cales, including >2 ka for the Kykula landslide (Pánek et al., 2010), 10^2 yr for the Smrdutá, Peklo and Pluskovec landslides and 10^{-1}–10^2 yr for the Lučovec landslide (Table 2, Fig. 2). The maintenance of anomalously high stream gradients after breaching the landslide dams was facilitated either by one massive blockage (e.g., Kykula landslide) or repeated damming of the same valley section due to recurrent slope failures (e.g., Lučovec, Peklo or Smrdutá landslides). Anomalous k_s values persist in particular valley stretches after the last breaching of the landslide dam; e.g., ~7.7 ka for the Kykula landslide (Pánek et al., 2010) or ~1.6 ka and ~0.5 ka for the Lučovec and Pluskovec landslides, respectively (Table 2, Fig. 2).

https://doi.org/10.1016/j.yqres.2013.03.009 Published online by Cambridge University Press

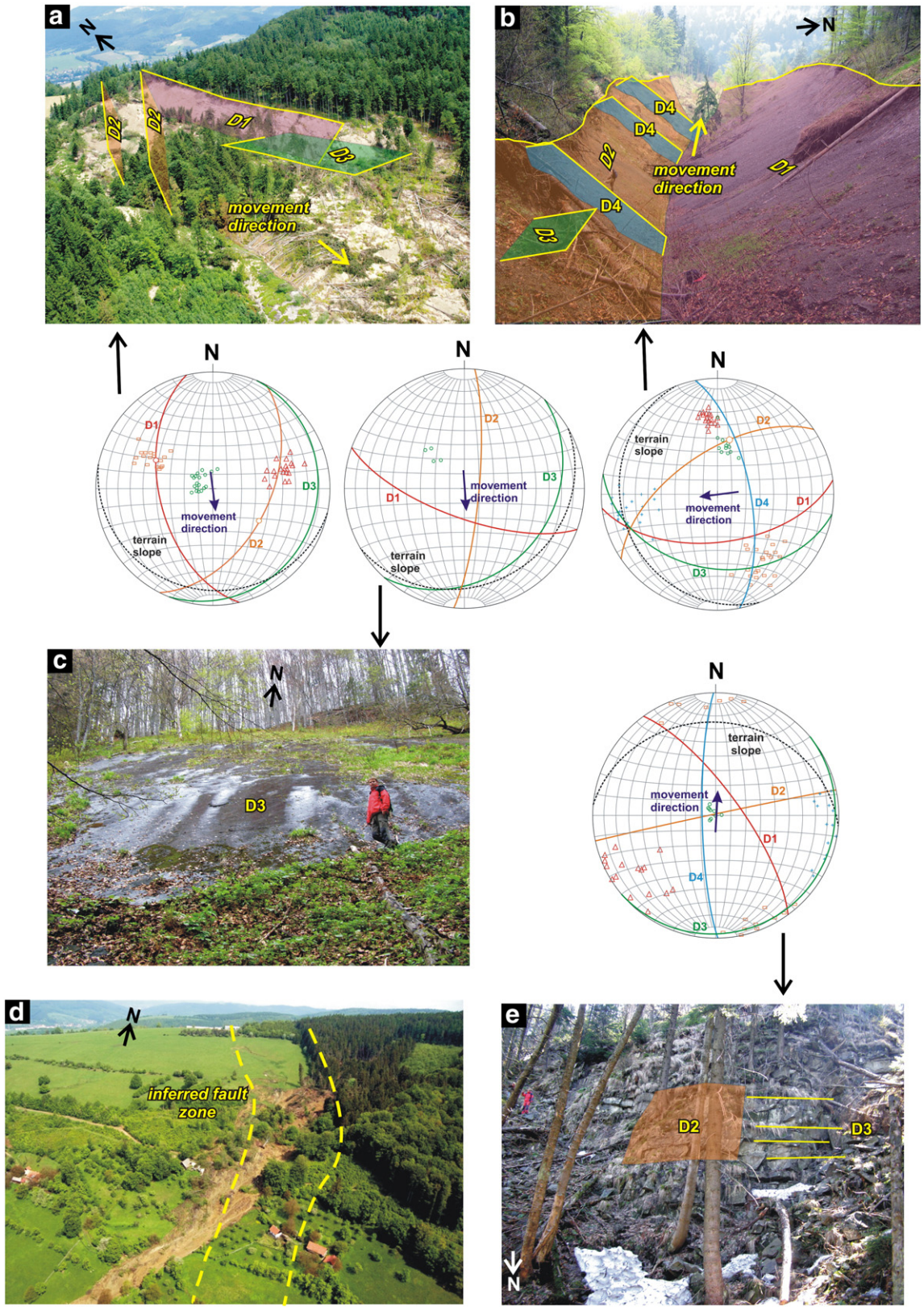

Figure 6. Types of structural preconditions exemplified by selected CFLLs from the studied area. a. Wedge-type headscarp predisposed by the intersection of two conjugate faults, D1 and D2 (May 2010 Girová landslide). b. Wedge-type headscarp predisposed by intersection of fault D2 with bedding planes, D1. c. Bedding planes D3 were partly responsible for translation of the Rycierova rockslide, which has a depletion zone predisposed by the intersection of two joint systems, D1 and D2. d. The April 2006 Hluboče landslide was most likely predisposed by a weakened tectonic shear zone. e. Strongly anisotropic sandstone beds (Godula Formation) in the headscarp area of the Ropice rockslide. The initial block of the landslide detached along the intersection of joint/fault system D2 and wedge-type arranged joints D1 and D4. Stereonets display great circles of the main discontinuity sets influencing or predisposing individual landslides.

https://doi.org/10.1016/j.yqres.2013.03.009 Published online by Cambridge University Press

Table 3
Timing and recurrence intervals for selected CFLLs.

Landslide	Available period[a] (cal ka BP)	Number of dated activations	Average recurrence interval (ka)[b]	Max. time interval between successive events[a]	Min. time interval between successive events[a]
Kykula	~11.5[c]–9.4	2	2.1	2.1	2.1
Peklo	~7.2–0.6	4	2.2	4	0.6
Girová	~7.4–AD 2010	4	2.5	5.9	0.6
Smrdutá	~4.6–0.3[d]	3	2.2	2.5	1.7
Lučovec	~1.7–0.8	3	0.4	0.7	0.2
Hošťálková	~1.4–AD 1919	2	1.4	1.4	1.4
Ropice	~1.4–0.4	2	1	1	1
Hluboče	~1.3–AD 2006	2	1.3	1.3	1.3
Malá Brodská	~1.1–AD 1997	2	1.1	1.1	1.1
Jezerné	~1.0–0.8	2	0.3	0.3	0.3

[a] Calculated from medians of calibrated radiocarbon ages.
[b] Calculated as p/n-1where p is the length of available period and n is a number of recurrences.
[c] Original calibrated radiocarbon age (12,860–12,670 cal yr BP) is too old and was corrected by pollen analysis.
[d] Original calibrated radiocarbon age (270–10 cal yr BP) is too young and was corrected by pollen analysis.

Discussion

Even though our CFLL dataset does not contain all examples of this phenomenon in the study region, this paper presents the most spectacular and well-investigated prehistoric and recent slope failures with liquefaction of displaced mass and catastrophic behaviour. The history of individual instabilities reveals that most landslides are recurrent features with time intervals between successive events on the order of 10^1–10^3 yr. An important issue for hazard planning is that debris released from some historic CFLLs have reached nearly the same position as previous events (e.g., Malá Brodská or Girová landslides); thus, some slope and valley-floor sections are particularly dangerous for human activities. Similar behaviour was observed for other long-runout landslides in British Columbia (Clague et al., 2003), the European Alps (Schlunegger et al., 2009) and Tien Shan (Sanhueza-Pino et al., 2011). CFLLs are important agents within denudation systems, evacuating debris from weakened sections of bedrock, and also contribute to controlling evolution of the valley network in the study area (Smolková, 2011).

Determining factors that control the time span between CFLL reactivations is important for hazard evaluation. Historical catastrophic

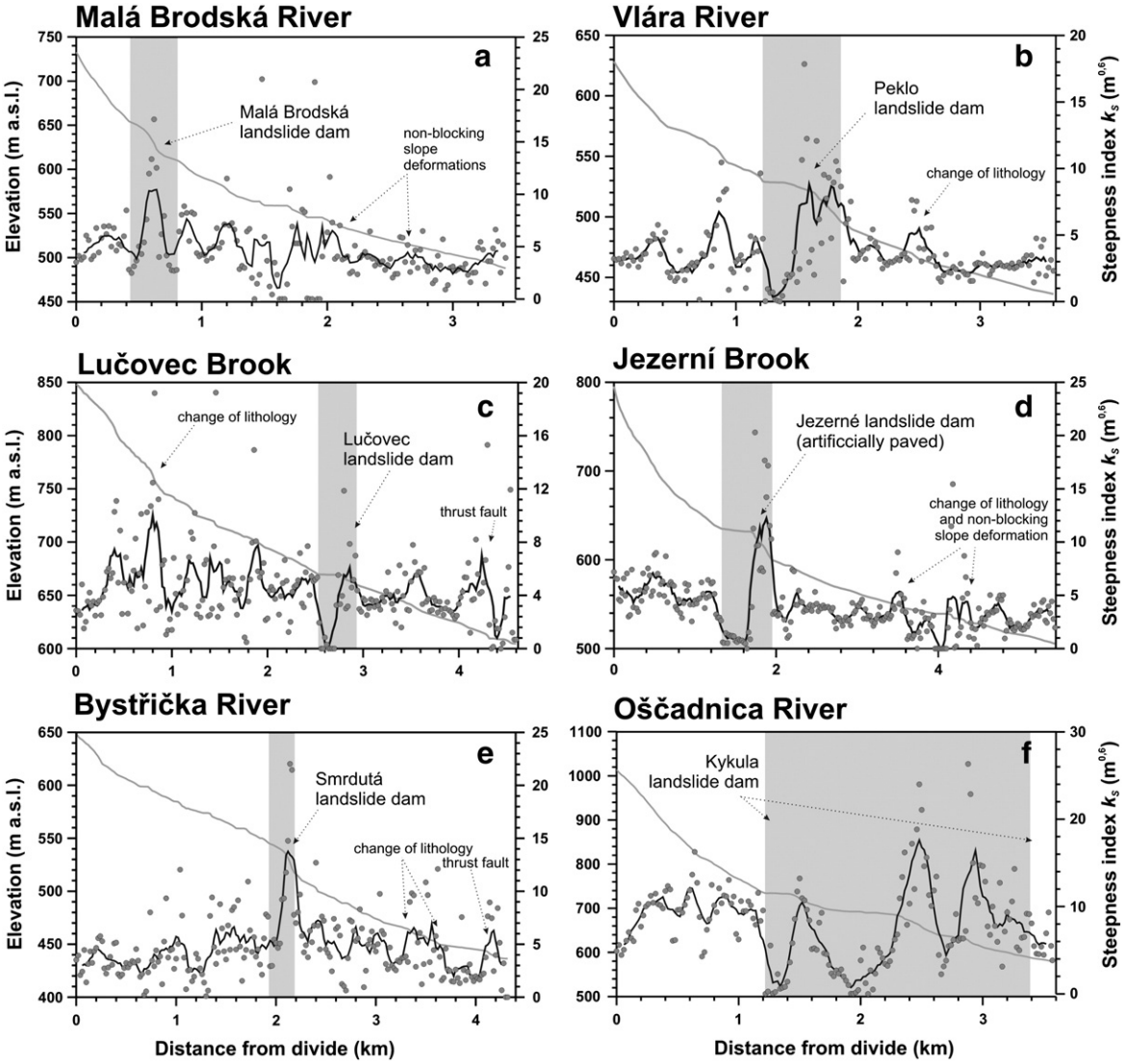

Figure 7. Influence of the selected CFLLs (grey boxes) on longitudinal profiles of the rivers (grey lines), expressed by the steepness index, k_S (grey dots), and its seven-point running mean (black lines) for the fixed concavity index $\theta = 0.3$. The highest values of k_S correspond spatially to landslide-dam breach channels, and the lowest values correspond to agradational segments above the damming.

https://doi.org/10.1016/j.yqres.2013.03.009 Published online by Cambridge University Press

landslides show that these events have originated during major hydrometeorological events, such as long-lasting and intensive rainfalls (e.g., in July 1997 (Rybář and Stemberk, 2000; Krejčí et al., 2002) and June 2010 (Baroň et al., 2011; Pánek et al., 2011a)) or rapid snowmelt accompanied by intensive rainfalls (e.g., March and April 2006 (Bíl and Müller, 2008; Klimeš et al., 2009)). While hydrometeorological extremes are immediate triggers of stability changes within rock massifs, the main factor controlling the recurrence interval is most likely the progressive strength degradation along major discontinuity sets (Kemeny, 2003). The pre-failure behaviour of catastrophic landslides is often characterised by creep movements within weakened bedrock. Three major recent catastrophic events of our dataset (i.e. January 1919 Hošťálková, March 2006 Hluboče and May 2010 Girová landslides) were preceded by several years of minor instability, as indicated by tension cracks in case of the Hošťálková landslide (Záruba, 1922). The Hluboče catastrophic earthflow in April 2006 was also the culmination of minor instabilities and hydrological changes within the slope, which were observable in the field and from aerial photographs at least six years before the event (Klimeš et al., 2009). As verified by dendrochronology, the May 2010 Girová landslide was preceded by at least 80 yr of accelerated creeping, which was concentrated along the future major headscarp (Pánek et al., 2011a).

Geomorphic evidence of prehistoric events, together with observations of recently collapsed landslides, reveals that slope instability recurrence occurs in three basic modes. The first type involves simple reactivation of the upper part of a precursory landslide (e.g., Hluboče or Malá Brodská earthflows). Even relatively small displacement of the source landslide, with an outcropping basal shear surface higher on the slope face, could lead to liquefaction and formation of a rapid earthflow (Klimeš et al., 2009). The second mode is represented by retrogressive failures shifting depletion areas upslope (e.g., the May 2010 Girová landslide). This evolution is most common with the presence of well-developed, pervasive discontinuities, such as wedge-type, composed conjugate faults (Fig. 3). As verified by electrical imaging of the May 2010 Girová catastrophic landslide (Pánek et al., 2011a), conjugate fault planes predisposing the headscarp form a several-metre-wide zone characterised by deeply weathered and weakened bedrock. In these cases, landslides migrate upslope, periodically consuming rock mass delimited by discontinuities, and this process usually terminates when the headscarp intersects the ridgeline. Chigira et al. (2003) described the Tsaoling landslide (Taiwan) and found that this type of retrogression even propagates upslope and affects portions of the slope that were not previously affected by any mass movements. The third mode of landslide recurrence is connected to the successive process of landslide rejuvenation with the reactivation of lower parts of slopes. This occurs when previous landslide activity overloads the central and lower portions of the slopes with debris and/or as a consequence of vertical erosion of streams unloading at the slope foot. This type of recurrence is represented by the Peklo landslide (and others; Table 1), which has reactivated several times since the Atlantic chronozone.

CFLLs have a significant influence on both mountain slope and valley floor topography in the study area. Due to the strong structural preconditions, failures are very often aligned with general topographical trends (i.e., direction of valleys and marginal slopes). In the western sector of the study area (Rača Unit), landslides often follow the general ENE–WSW nature of the Magura Nappe, especially in the zones of weak rocks. In these conditions, narrow, wedge type landslide depletion zones are assumed to be potential areas for the future drainage network (e.g., Malá Brodská, Peklo and Slopné landslides), but similar development could also be expected for other slope failures. The time-persistent topographic signal recorded within long profiles of valleys underlines the recurrent character of CFLLs acting on given slope sections for long time periods (Fig. 7).

Dating of individual CFLLs and their reactivations indicates that these mass movements originated throughout the Holocene period. The largest landslides originated both at the beginning (ca. 11.5 cal ka BP old Kykula landslide, with volume ~12×10^6 m^3 — largest landslide) and end (the May 2010 Girová landslide, with volume ~2.5×10^6 m^3 — second largest landslide) of the observed time period. This pattern suggests that gross conditions influencing slope stability and activation of CFLLs are relatively similar throughout the Holocene, with higher event probabilities during more humid climatic oscillations (Fig. 8). Our dataset (25 dated landslide events) is too limited for chronological determinations, but it shows a possible correlation with other central-European paleoclimatological proxy records, including lake-level high stands (Magny, 2004), δ^{18}O speleothem records

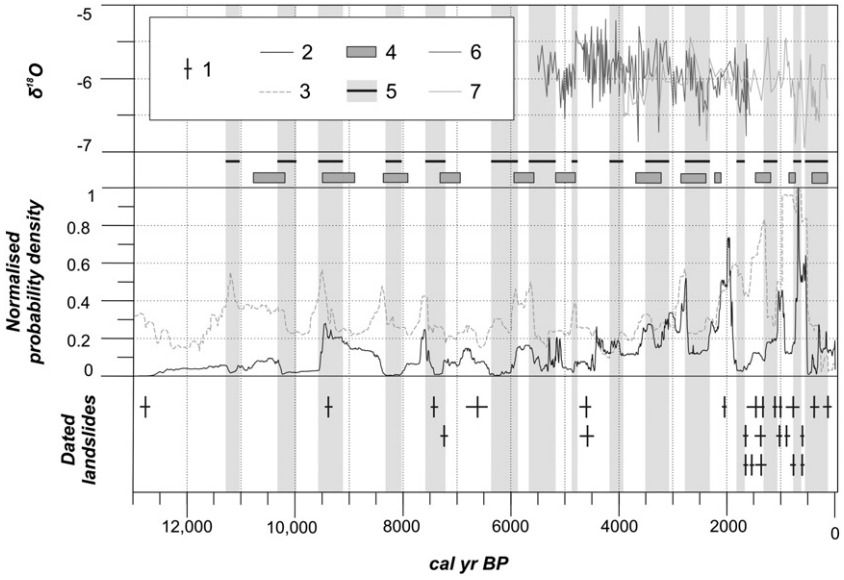

Figure 8. Dating of individual CFLLs and their reactivations compared to probability density curve of Holocene dated landslide events in the Czech and Polish part of the Outer Western Carpathians and other central-European paleoclimatological proxy records: (1) single dates of studied CFLLs (median ± 1σ), 25 dates (this study; Baroň, 2007; Klimeš et al., 2009; Pánek et al., 2009a,b, 2010; Baroň et al., 2011; Pánek et al., 2011a, 2013); (2) normalised probability density curve of the Czech and Polish landslide events, 85 dates (Alexandrowicz and Alexandrowicz, 1999; Margielewski, 2006a; Baroň, 2007; Margielewski et al., 2010, 2011); (3) normalised probability density curve of the hydrological events in Polish rivers, 331 dates (Starkel et al., 2006); (4) advances of Alpine glaciers (by various authors in Starkel et al., 2006); (5) mid-European higher lake-level phases (Magny, 2004); (6) δ^{18}O record from stalagmites AH-1 and (7) B7-7 in Sauerland/Germany (Niggemann et al., 2003).

https://doi.org/10.1016/j.yqres.2013.03.009 Published online by Cambridge University Press

(Niggemann et al., 2003), Alpine glacial advances (various authors in Starkel et al., 2006), paleofloods (Notebaert and Verstraeten, 2010; Starkel et al., 2006) and timing of other landslides from the Czech and Polish flysch Carpathians (Baroň et al., 2004; Margielewski, 2006a; Margielewski et al., 2011) (Fig. 8).

The largest dated failure (Kykula landslide) originated during several phases between ca. 11.5–9.4 cal ka BP, i.e. in the period of major climatic change and restoration of water circulation within slopes after permafrost degradation at the beginning of the Holocene period (Starkel et al., 2007). This stage is characterised by a large number of dated landslides in the Carpathians (Margielewski, 2006a) and Alps (Soldati et al., 2004; Borgatti and Soldati, 2010). A few CFFLs fall within the interval 7.5–4.6 cal ka BP corresponding with exceptionally humid conditions of the Atlantic chronozone between 7.4 and 6.3 cal ka BP (Kalis et al., 2003) and the onset of the Subboreal chronozone (ca. 4.6 cal ka BP; Niggemann et al., 2003; Starkel et al., 2006; Notebaert and Verstraeten, 2010) (Fig. 8).

More than 50% of our dated landslides and reactivations (14 events) occurred within the Subatlantic period, 2–0.8 cal ka BP (Fig. 8). This period coincides with two stages of lake-level high stands in the Alps at 1.8–1.7 and 1.3–1.1 cal ka BP (Magny, 2004), as well as with three stages of increased flood frequencies at 2.1–1.7, 1.5–1.3 and 1–0.6 cal ka BP (Fig. 7; Starkel et al., 2006). A pronounced peak of dated CFLLs (34%) is connected to a relatively short period between 1.7 and 1 cal ka BP relating to a humid stage represented by large floods in various Central European rivers (Notebaert and Verstraeten, 2010; Starkel et al., 2006) and lake-level high stand of the Alpine lakes (Magny, 2004). Highly skewed temporal distribution of CFLLs biased to the Subatlantic chronozone is most likely determined by erosion of older landslides and/or burial of ancient accumulations by debris coming from the latest stages of mass movement activity. Bias in our dataset is partly caused by types of the studied landslides, i.e. highly mobile failures with large erosive potential. In contrast to our study, a large number of predominantly short-displacement rotational bedrock landslides was dated in the Czech Carpathians by Baroň et al. (2004) and in the Polish Carpathians by Margielewski (2006a) to earlier stages of the Holocene.

Conclusion

Thirteen examples of recent and prehistoric Holocene CFLLs were detected in the western part of the Flysch Carpathians (Czech Republic, Slovakia). They are mostly comprised of structurally predisposed failures nested within chronic, slow-moving DSGSDs. They also usually consist of a deep-seated landslide in the upper portion, which, due to its basal slip surface outcropping in the slope face, are transformed into earthflows due to liquefaction. Most of the failures were recurrent features, repeating on the same slopes on time intervals of 10^1–10^3 yr, with most recurrences at ca. 1–2 ka. Dated events occurred during humid phases of the Younger Dryas/Holocene transition (11.5–9.4 cal ka BP), Atlantic chronozone (7.4–6.6 cal ka BP), the beginning of the Subboreal chronozone (ca. 4.6 cal ka BP) and, primarily, within the Subatlantic chronozone at ca. 2–0.8 cal ka BP (>50% of all events). This study suggests that slopes underlain by an unfavourable structural setting and affected by long-term DSGSDs may produce CFLLs, even if they are located in the medium-high mountains.

Acknowledgments

This research was supported by the Czech Science Foundation project GAP209/10/0309: "The effect of historical climatic and hydrometeorological extremes on slope and fluvial processes in the Western Beskydy Mts and their forefield," by the Czech Geological Survey project 215124–2: "Investigation and monitoring of slope failures on territory of the Czech Republic — ISPROFIN" and by the University of Ostrava Foundation project SGS04/PřF/2012. Thanks are extended to Petr Tábořík for assistance during field work and editor Alan Gillespie and two anonymous reviewers for valuable comments that substantially improved the manuscript.

References

Alexandrowicz, S.W., Alexandrowicz, Z., 1999. Recurrent Holocene landslides: a case study of the Krynica landslide in the Polish Carpathians. The Holocene 9, 91–99.
Baroň, I., 2007. Results of radiocarbon dating of deep-seated landslides in the area of Vsetín and Frýdek-Místek districts. Geologické výzkumy na Moravě a ve Slezsku 14, 10–12 (in Czech with English abstract).
Baroň, I., Cílek, V., Krejčí, O., Melichar, R., Hubatka, F., 2004. Structure and dynamics of deep-seated slope failures in the Magura Flysch Nappe, Outer Western Carpathians (Czech Republic). Natural Hazards and Earth System Sciences 4, 549–562.
Baroň, I., Agliardi, F., Ambrosi, Ch., Crosta, G.B., 2005. Numerical analysis of deep-seated mass movements in the Magura Nappe; Flysch Belt of the Western Carpathians (Czech Republic). Natural Hazards and Earth System Sciences 5, 367–374.
Baroň, I., Baldík, V., Fifernová, M., 2010. Preliminary assessment of a recent denudation rate of the Flysch Belt of Outer West Carpathians — case study: Bystřička River catchment in Vsetínské Hills. Geologické výzkumy na Moravě a ve Slezsku 17, 10–13 (in Czech with English abstract).
Baroň, I., Řehánek, T., Vošmík, J., Musel, V., Kondrová, L., 2011. Report on a recent deep-seated landslide at Gírová Mt., Czech Republic, triggered by a heavy rainfall: the Gírová Mt., Outer West Carpathians; Czech Republic. Landslides 8, 355–361.
Bertolini, G., Casagli, N., Ermini, L., Malaguti, C., 2004. Radiocarbon data on Lateglacial and Holocene landslides in the Northern Apennines. Natural Hazards 31, 645–662.
Biely, A. (ed.), 1996. Geological map of the Slovak Republic 1: 500 000. Geologická služba Slovenskej republiky, Bratislava [in Slovak].
Bíl, M., Müller, I., 2008. The origin of shallow landslides in Moravia (Czech Republic) in the spring 2006. Geomorphology 99, 246–253.
Bookhagen, B., Thiede, R.C., Strecker, M.R., 2005. Late Quaternary intensified monsoon phases control landscape evolution in the northwest Himalaya. Geology 33, 149–152.
Borgatti, L., Soldati, M., 2010. Landslides as a geomorphological proxy for climate change: a record from the Dolomites (northern Italy). Geomorphology 120, 56–64.
Brideau, M.A., Yan, M., Stead, D., 2009. The role of tectonic damage and brittle rock fracture in the development of large rock slope failures. Geomorphology 103, 30–49.
Bronk Ramsey, C., 2009. Bayesian analysis of radiocarbon dates. Radiocarbon 51, 337–360.
Cháb, J., Stráník, Z., Eliáš, M., 2007. Geological map of the Czech Republic 1: 500 000. Česká geologická služba, Praha (in Czech).
Chigira, M., Wang, W.N., Furuya, T., Kamai, T., 2003. Geological causes and geomorphological precursors of the Tsaoling landslide triggered by the 1999 Chi-Chi earthquake, Taiwan. Engineering Geology 68, 259–273.
Clague, J.J., Friele, P.A., Hutchinson, I., 2003. Chronology and hazards of large debris flows in the Cheekye River basin, British Columbia, Canada. Environmental and Engineering Geoscience 9, 99–115.
Corominas, J., Moya, J., 2008. A review of assessing landslide frequency for hazard zoning purposes. Engineering Geology 102, 193–213.
Cruden, D.M., Varnes, D.J., 1996. Landslide types and processes. In: Turner, A.K., Shuster, R.L. (Eds.), Landslides: Investigation and Mitigation. Transportation Research Board, Washington DC, pp. 36–75.
Danišík, M., Pánek, T., Matýsek, D., Dunkl, I., Frisch, W., 2008. Apatite fission track and (U–Th)/He dating of teschenite intrusions gives time constraints on accretionary processes and development of planation surfaces in the Outer Western Carpathians. Zeitschrift für Geomorphologie 52, 273–289.
Dortch, J.M., Owen, L.A., Haneberg, W.C., Caffee, M.W., Dietsch, C., Kamp, U., 2009. Nature and timing of large landslides in the Himalaya and Transhimalaya of northern India. Quaternary Science Reviews 28, 1037–1054.
Evans, S.G., Roberts, N.J., Ischuk, A., Delaney, K.B., Morozova, G.S., Tutubalina, O., 2009. Landslides triggered by the 1949 Khait earthquake, Tajikistan, and associated loss of life. Engineering Geology 109, 195–212.
Flint, J.J., 1974. Stream gradient as a function of order, magnitude, and discharge. Water Resources Research 10, 969–973.
Guzzetti, F., Reichenbach, P., Cardinali, M., Galli, M., Ardizzone, F., 2005. Probabilistic landslide hazard assessment at the basin scale. Geomorphology 72, 272–299.
Guzzetti, F., Ardizzone, F., Cardinali, M., Rossi, M., Valigi, D., 2009. Landslide volumes and landslide mobilization rates in Umbria, central Italy. Earth and Planetary Science Letters 279, 222–229.
Hancox, G.T., McSaveney, M.J., Manville, V.R., Davies, T.R., 2005. The October 1999 Mt Adams rock avalanche and subsequent landslide dam-break flood and effects in Poerua River, Westland, New Zealand. New Zealand Journal of Geology and Geophysics 48, 683–705.
Kalis, A.J., Merkt, J., Wunderlich, J., 2003. Environmental changes during the Holocene climatic optimum in central Europe — human impact and natural causes. Quaternary Science Reviews 22, 33–79.
Kemeny, J., 2003. The time-dependent reduction of sliding cohesion due to rock bridges along discontinuities: a fracture mechanics approach. Rock Mechanics and Rock Engineering 36, 27–38.
Klimeš, J., Baroň, I., Pánek, T., Kosačík, T., Burda, J., Kresta, F., Hradecký, J., 2009. Investigation of recent catastrophic landslides in the flysch belt of Outer Western Carpathians (Czech Republic): progress towards better hazard assessment. Natural Hazards and Earth System Sciences 9, 119–128.

https://doi.org/10.1016/j.yqres.2013.03.009 Published online by Cambridge University Press

Korup, O., 2006. Rock-slope failure and the river long profile. Geology 34, 45–48.
Korup, O., McSaveney, M.J., Davies, T.R.H., 2004. Sediment generation and delivery from large historic landslides in the Southern Alps, New Zealand. Geomorphology 61, 189–207.
Korup, O., Montgomery, D.R., Hewitt, K., 2010. Glacier and landslide feedbacks to topographic relief in the Himalayan syntaxes. Proceedings of the National Academy of Sciences 107, 5317–5322.
Krejčí, O., Baroň, I., Bíl, M., Hubatka, F., Jurová, Z., Kirchner, K., 2002. Slope movements in the Flysch Carpathians of Eastern Czech Republic triggered by extreme rainfalls in 1997: a case study. Physics and Chemistry of the Earth 27, 1567–1576.
Lang, A., Moya, J., Corominas, J., Schrott, L., Dikau, R., 1999. Classic and new dating methods for assessing the temporal occurrence of mass movements. Geomorphology 30, 33–52.
Lenhardt, W.A., Švancara, J., Melichar, P., Pazdírková, J., Havíř, J., Sýkorová, Z., 2007. Seismic activity of the Alpine–Carpathian–Bohemian Massif region with regard to geological and potential field data. Geologica Carpathica 58, 397–412.
Lopez Saez, J., Corona, C., Stoffel, M., Schoeneich, P., Berger, F., 2012. Probability maps of landslide reactivation derived from tree-ring records: Pra Bellon landslide, southern French Alps. Geomorphology 138, 189–202.
Magny, M., 2004. Holocene climate variability as reflected by mid-European lake-level fluctuations and its probable impact on prehistoric human settlements. Quaternary International 113, 65–79.
Margielewski, W., 2006a. Records of the Late Glacial–Holocene palaeoenvironmental changes in landslide forms and deposits of the Beskid Makowski and Beskid Wyspowy Mts. Area (Polish Outer Carpathians). Folia Quaternaria 76, 1–149.
Margielewski, W., 2006b. Structural control and types of movements of rock mass in anisotropic rocks: case studies in the Polish Flysch Carpathians. Geomorphology 77, 47–68.
Margielewski, W., Krąpiec, M., Valde-Nowak, P., Zernitskaya, V., 2010. A Neolithic yew bow in the Polish Carpathians: evidence of the impact of human activity on mountainous palaeoenvironment from the Kamiennik landslide peat bog. Catena 80, 141–153.
Margielewski, W., Kołaczek, P., Michzcyński, A., Obidowicz, A., Pazdur, A., 2011. Record of the meso-and neoholocene palaeoenvironmental changes in the Jesionowa landslide peat bog (Beskid Sądecki Mts. Polish Outer Carpathians). Geochronometria 38, 138–154.
Niggemann, S., Mangini, A., Mudelsee, M., Richter, D.K., Wurth, G., 2003. Sub-Milankovitch climatic cycles in Holocene stalagmites from Sauerland, Germany. Earth and Planetary Science Letters 216, 539–547.
Notebaert, B., Verstraeten, G., 2010. Sensitivity of West and Central European river systems to environmental changes during the Holocene: a review. Earth-Science Reviews 103, 163–182.
Pánek, T., Smolková, V., Hradecký, J., Šilhán, K., 2009a. Late Holocene evolution of landslides in the frontal part of the Magura Nappe: Hlavatá Ridge, Moravian–Silesian Beskids (Czech Republic). Moravian Geographical Reports 17, 2–11.
Pánek, T., Hradecký, J., Minár, J., Hungr, O., Dušek, R., 2009b. Late Holocene catastrophic slope collapse affected by deep-seated gravitational deformation in flysch: Ropice Mountain, Czech Republic. Geomorphology 103, 414–429.
Pánek, T., Hradecký, J., Smolková, V., Šilhán, K., Minár, J., Zernitskaya, V., 2010. The largest prehistoric landslide in northwestern Slovakia: chronological constraints of the Kykula flow-like landslide and related dammed lakes. Geomorphology 120, 233–247.
Pánek, T., Šilhán, K., Tábořík, P., Hradecký, J., Smolková, V., Lenart, J., Brázdil, R., Kašičková, L., Pazdur, A., 2011a. Catastrophic slope failure and its origins: case of the May 2010 Girová Mountain flow-like rockslide (Czech Republic). Geomorphology 130, 352–364.
Pánek, T., Tábořík, P., Klimeš, J., Komárková, V., Hradecký, J., Šťastný, M., 2011b. Deep-seated gravitational slope deformations in the highest parts of the Czech Flysch Carpathians: evolutionary model based on kinematic analysis, electrical imaging and trenching. Geomorphology 129, 92–112.
Pánek, T., Smolková, V., Hradecký, J., Sedláček, J., Zernitskaya, V., Kadlec, J., Pazdur, A., Řehánek, T., 2013. Late-Holocene evolution of a floodplain impounded by the Smrdutá landslide, Carpathian Mountains (Czech Republic). The Holocene 23, 218–229.
Picha, F.J., Stráník, Z., Krejčí, O., 2006. Geology and hydrocarbon resources of the Outer Western Carpathians and their foreland, Czech Republic. In: Golonka, J., Picha, F.J. (Eds.), The Carpathians and Their Foreland: Geology and Hydrocarbon Resources. The American Association of Petroleum Geologists. Tulsa, Oklahoma, pp. 49–175.
Prager, C., Ivy-Ochs, S., Ostermann, M., Synal, H.-A., Patzelt, G., 2009. Geology and radiometric ^{14}C-, ^{36}Cl- and Th-/U-dating of the Fernpass rockslide (Tyrol, Austria). Geomorphology 103, 93–103.
Reimer, P.J., Baillie, M.G.L., Bard, E., Bayliss, A., Beck, J.W., Blackwell, P.G., Bronk Ramsey, C., Buck, C.E., Burr, G.S., Edwards, R.L., Friedrich, M., Groothes, P.M., Guilderson, T.P., Hajdas, I., Heaton, T.J., Hogg, A.G., Hughen, K.A., Kaiser, K.F., Kromer, B., McCormac, F.G., Manning, S.W., Reimer, R.W., Richards, D.A., Southon, J.R., Talamo, S., Turney, C.S.M., Van Der Plicht, J., Weyhenmayer, C.E., 2009. IntCal09 and Marine09 radiocarbon age calibration curves, 0–50,000 years cal BP. Radiocarbon 51, 1111–1150.
Rybář, J., Stemberk, J., 2000. Avalanche-like occurrences of slope deformations in the Czech Republic and coping with their consequences. Landslide News 13, 28–33.
Sanhueza-Pino, K., Korup, O., Hetzel, R., Munack, H., Weidinger, J.T., Dunning, T., Ormukov, Ch., Kubik, P.W., 2011. Glacial advances constrained by ^{10}Be exposure dating of bedrock landslides, Kyrgyz Tien Shan. Quaternary Research 76, 295–304.
Schlunegger, F., Badoux, A., Mc Ardell, B.W., Gwerder, C., Schnydrig, D., Rieke-Zapp, D., Molnar, P., 2009. Limits of sediment transfer in an alpine debris-flow catchment, Illgraben, Switzerland. Quaternary Science Reviews 28, 1097–1105.
Šimeková, J., Martinčeková, T., 2006. Atlas of Slope Stability Maps, Slovakia, 1:50 000. INGEO ighp, Žilina, Slovak Republic [in Slovak].
Smolková, V., 2011. Slope Deformations and their Impact on Valley Bottom Development (in the Czech Part of the Carpathians). (PhD thesis) University of Ostrava, Ostrava (134 pp. [in Czech with English abstract]).
Soldati, M., Corsini, A., Pasuto, A., 2004. Landslides and climate change in the Italian Dolomites. Catena 55, 141–161.
Starkel, L., Soja, R., Michczyńska, D.J., 2006. Past hydrological events reflected in Holocene history of Polish rivers. Catena 66, 24–33.
Starkel, L., Gębica, P., Superson, J., 2007. Last Glacial–Interglacial cycle in the evolution of river valleys in southern and central Poland. Quaternary Science Reviews 26, 2924–2936.
Whipple, K.X., 2004. Bedrock rivers and the geomorphology of active orogens. Annual Review of Earth and Planetary Sciences 32, 151–185.
Záruba, Q., 1922. Study on landslide terrains in the Vsetín and Vallachian Region. Práce z geologického ústavu čes. vys. učení technického v Praze, pp. 170–177 (in Czech).
Zattin, M., Andreucci, B., Jankowski, L., Mazzoli, S., Szaniawski, R., 2011. Neogene exhumation in the Outer Western Carpathians. Terra Nova 23, 283–291.

https://doi.org/10.1016/j.yqres.2013.03.009 Published online by Cambridge University Press